5-aminiolevulinic acid induces a radiodynamic effect with enhanced delayed reactive oxygen species production under hypoxic conditions in lymphoma cells: An *in vitro* study

KOHEI SUZUKI, JUNKOH YAMAMOTO, KEITA TOH and RYO MIYAOKA

Department of Neurosurgery, University of Occupational and Environmental Health, Kitakyushu, Fukuoka 807-8555, Japan

Received January 20, 2023; Accepted April 6, 2023

DOI: 10.3892/etm.2023.12059

Abstract. Primary central nervous system lymphoma (PCNSL) is a rare and aggressive type of intracranial tumor. However, PCNSL is radiosensitive; thus, whole-brain radiotherapy (WBRT) is often selected as an alternative consolidation therapy. WBRT-related delayed neurotoxicity can affect the quality of life of the elderly. 5-aminolevulinic acid (ALA) is a natural precursor of heme and has been widely used as a live molecular fluorescence marker in brain tumor surgery. Experimental studies have demonstrated that combination therapy with 5-ALA and ionizing irradiation (IR), denoted radiodynamic therapy (RDT), resulted in tumor suppression in cancer, including glioma, melanoma, colorectal cancer, prostate cancer, breast cancer and lung cancer; however, to the best of our knowledge, this method has not been investigated in lymphoma. The present study aimed to investigate the radiodynamic effect of 5-ALA on lymphoma cells *in vitro*. The synthesis of 5-ALA-induced protoporphyrin IX (PpIX) was assessed under normal and hypoxic conditions in lymphoma cells (Raji, HKBML and TK). Subsequently, the radiodynamic effect of 5-ALA was evaluated using a colony formation assay and reactive oxygen species (ROS) production after RDT was examined using flow cytometry. Finally, the mitochondrial density in the lymphoma cells was evaluated. Lymphoma cells exhibited a high accumulation of 5-ALA-induced PpIX in the flow cytometric analysis, and a decrease in the surviving fraction under IR in cells with 5-ALA treatment compared with cells not treated with 5-ALA in the colony formation assay under normal and hypoxic conditions. Although ROS production 12 h after IR was increased compared with that immediately after IR (0 h), pretreatment with 5-ALA enhanced the delayed ROS production in each lymphoma cell line under normoxic conditions. Raji and TK cells exhibited an increase in ROS production 12 h after IR compared with that at 0 h in the 5-ALA-untreated cells under hypoxic conditions. Raji, HKBML and TK cells exhibited an increase in ROS production 12 h after IR compared with that at 0 h in the 5-ALA-treated cells, while TK cells exhibited enhancement of ROS production 12 h after IR in 5-ALA-treated cells compared with 5-ALA-untreated cells under hypoxic conditions. Other studies have demonstrated that impaired mitochondria damaged by IR produce ROS via the metabolic process, then damage the rest of the surrounding normal mitochondria, consequently propagating oxidative stress within tumor cells and leading to cell death. Thus, we hypothesized that the propagating oxidative stress after IR was associated with mitochondrial density in tumor cells. Namely, high accumulation of 5-ALA-indcued PpIX may promote ROS production in mitochondria of tumor cells after IR, and suppress the cell surviving fraction via the propagation of oxidative stress. In the colony formation assay, Raji cell colony formation was suppressed by RDT with 5-ALA. Simultaneously, the mitochondrial density in the Raji cells was higher than that in other cell lines. Pretreatment with 5-ALA enhanced delayed ROS production after IR in lymphoma cells under normoxic conditions. Under hypoxic conditions, only TK cells exhibited enhancement of ROS production 12 h after IR in the 5-ALA-treated group compared with the 5-ALA-untreated group. Although further studies evaluating the effect of hypoxic conditions in lymphoma cells are needed, the results suggested that RDT with 5-ALA could suppress colony formation under normal and hypoxic conditions in lymphoma cells. Therefore, RDT with 5-ALA is a potential treatment option for PCNSL.

Correspondence to: Dr Junkoh Yamamoto, Department of Neurosurgery, University of Occupational and Environmental Health, 1-1 Iseigaoka, Yahatanishi-ku, Kitakyushu, Fukuoka 807-8555, Japan
E-mail: yama9218@med.uoeh-u.ac.jp

Abbreviations: PCNSL, primary central nervous system lymphoma; WBRT, whole-brain radiotherapy; 5-ALA, 5-aminolevulinic acid; PpIX, protoporphyrin IX; ROS, reactive oxygen species; RDT, radiodynamic therapy; DCFD, 2CM-H_2DCFDA; HIF, hypoxia-induced factor; FBS, fetal bovine serum; MFI, median fluorescence intensity; IR, ionizing irradiation

Key words: RDT, PCNSL, 5-ALA, hypoxia, radiation, mitochondria, ROS, hemtological malignancy

Introduction

Primary central nervous system lymphoma (PCNSL) is a rare and aggressive intracranial tumor that accounts for approximately 2% of all primary central nervous system tumors. PCNSL has an overall incidence rate of 0.43 per 100,000

people and a slight predilection for men (1). In particular, the incidence of PCNSL has increased in patients over 70 years (2). PCNSL is composed of diffuse large B-cell lymphoma (DLBCL), which is the most common histopathological subtype (90-95%), followed by Burkitt (5%), lymphoblastic (5%), marginal zone (3%), and T-cell lymphoma (2-3%) (3).

In general, PCNSL tumors are sensitive to radiotherapy and chemotherapy. High-dose methotrexate (MTX)-based multiple chemotherapy, including rituximab and cytarabine, has been used as a standard induction therapy in young patients, and elderly patients who have multiple comorbidities with renal and bone marrow dysfunction require a reduction in doses of methotrexate (2,4). Considering the high radiosensitivity of PCNSL, whole-brain radiotherapy (WBRT) is often selected as an alternative consolidation therapy to high-dose chemotherapies. However, delayed WBRT-related neurotoxicity effects, such as severe cognitive dysfunction, affect the quality of life of survivors and are observed more frequently in the elderly (2). Thus, WBRT tends to be deferred until tumor recurrence or administered with a reduced irradiation dose to avoid WBRT-related delayed neurotoxicity in the elderly. The median survival of patients with PCNSL over 70 years of age has not changed in the last few decades and remains in the range of 6-7 months (2). Although PCNSL is radiosensitive, radiosensitizers have the potential to reduce the irradiation dose, avoid delayed neurotoxicity, and maintain the therapeutic effect of radiotherapy for PCNSL. Therefore, new drug development for radiosensitizers is essential in PCNSL.

5-aminolevulinic acid (ALA) is a natural precursor of heme (5). In the final step of heme synthesis in the mitochondria, Fe^{2+} is inserted into protoporphyrin IX (PpIX) to form heme. 5-ALA is rapidly converted to heme in normal cells, whereas in various tumor cells, PpIX is not converted to heme; consequently, PpIX selectively and highly accumulates in the mitochondria of tumor cells (5). 5-ALA-induced PpIX is also a photosensitizer and exhibits high tumor selectivity. Thus, 5-ALA has been widely used as a live molecular fluorescence marker for brain tumor surgery, denoted photodynamic diagnosis, for malignant gliomas (6), meningiomas (7) and PCNSL (8). In a clinical study of stereotaxic biopsy for intracranial lymphomas, histopathological analysis showed that all samples with 5-ALA fluorescence (strong and vague) contained diagnostic lymphoma tissue, resulting in a positive predictive value of 100% (8).

A previous study demonstrated that PpIX could enhance the production of reactive oxygen species (ROS) such as superoxide, singlet oxygen, and hydroxyl radicals via water radiolysis induced by ionizing irradiation (IR) (9). We confirmed that radiotherapy with 5-ALA administration enhanced mitochondrial ROS production and host antitumor response in glioma *in vitro* and *in vivo* (10-13). This combination therapy is known as radiodynamic therapy (RDT), and recent experimental studies have demonstrated the efficacy of RDT using 5-ALA in various cancer cells, including melanoma (14), colorectal cancer (15), prostate cancer (16), breast cancer (17) and lung cancer (18) cells *in vitro* and *in vivo*. Therefore, we hypothesized that tumors that accumulate 5-ALA-induced PpIX are candidates for RDT. Although previous studies on 5-ALA/RDT focused on radioresistant malignant neoplasms, no study focused on radiosensitive malignant neoplasms such as hematological malignancies.

In the present study, we assessed the synthesis of 5-ALA-induced PpIX and its radiodynamic effect under normal and hypoxic conditions in lymphoma cells. We then evaluated lymphoma cells' intracellular ROS production after exposure to IR. We also discuss the possible mechanism of the radiodynamic effect of 5-ALA in lymphoma cells and the potential of 5-ALA as a radiosensitizer for PCNLS.

Materials and methods

Data collection. The present study was conducted at the Department of Neurosurgery, University of Occupational and Environmental Health, from January 2021 to July 2022.

Chemicals. 5-ALA was purchased from Cosmo Bio Co. Ltd (Tokyo, Japan). It was then dissolved in fresh culture medium at a final concentration of 1 μM for intracellular PpIX imaging and 0.3 μM for other *in vitro* studies. Among other materials, 2CM-H_2DCFDA (DCFD) and Thiazolyl Blue tetrazolium bromide were purchased from Sigma-Aldrich (Tokyo, Japan) and Invitrogen (CA, USA), and MitoTracker Deep Red FM and NucBlue™ Live Cell Stain were purchased from Thermo Fisher Scientific, Inc. (Waltham, MA, USA). The DCFD was dissolved in Hank's Balanced Salt Solution with calcium and magnesium and without red phenol 1X (Invitrogen) at a final concentration of 10 μM. In addition, the MitoTracker Deep Red FM was dissolved in fresh culture medium at a final concentration of 50 nM, while the Thiazolyl Blue tetrazolium bromide was dissolved in PBS (-) at a final concentration of 5 mg/ml.

Culture and treatment of cells. A human Burkitt lymphoma cell line (Raji) and two human brain lymphoma cell lines (HKBML and TK) were used. The Raji and HKBML lines were obtained from the ATCC and RIKEN BRC Cell Bank, respectively, while the TK cell line was obtained from the JCRB cell bank. Raji and TK cells were cultured for several days in RPMI-1640 supplemented with 10% fetal bovine serum (FBS), while the HKBML line was cultured in Ham's F12 supplemented with 15% FBS at 37˚C before use. The cell lines were maintained in a humidified incubator with 5% CO_2 at 37˚C. Hypoxic conditions were induced by placing the cells in a multi-gas incubator with 5% O_2/balanced N_2 for 24 h just before each experiment at 37˚C. Finally, 5-ALA was dissolved in each medium and incubated with the cell lines for 4 h under normoxic and hypoxic conditions.

Flow cytometric analysis. After each incubation period, cells were collected by centrifugation (800 x g for 5 min at 4˚C). Immediately afterwards, the cells were re-suspended in cold PBS/FBS and analyzed using a flow cytometer (EC800; Sony Biotechnology, Tokyo, Japan). Overall, $3x10^6$ cells from each sample were evaluated. Analyses of flow cytometric data were performed using FlowJo software (Tree Star Inc., Ashland, OR, USA). The median fluorescence intensity (MFI) of 5-ALA-induced PpIX was relative to that of untreated cells in each cell line, and then, the relative MFI of 5-ALA-induced

PpIX was compared in normoxic and hypoxic conditions, as described previously (13).

Evaluation of PpIX fluorescence intensity in lymphoma cells. Lymphoma cells were seeded in 35-mm culture flasks and cultured in complete medium containing 0.3 μM 5-ALA for 4 h. After 5-ALA treatment, the cells were immediately assessed using a flow cytometer (excitation, 488 nm; emission, 640/30 nm band-pass filter). The control cells were not exposed to 5-ALA under normoxic conditions. The MFI of PpIX for the treated cells relative to that of the 5-ALA-untreated cells was calculated for each cell line using FlowJo software.

Simple Western experiments. We used the Simple Western system (ProteinSimple, Inc., CA, USA), a non-gel-based and western blot-like substitute, to efficiently and quantitatively analyze the protein expression levels of the cells (19,20). Whole protein lysates were obtained by re-suspending cell pellets in RIPA buffer (WAKO Pure Chemical Co., Osaka, Japan, 182-02451) with a Halt protease inhibitor cocktail kit (Thermo Fisher Scientific, 78410), and the final concentration was standardized to 0.75 μg/ml. Simple western blot analyses were performed with HIF1α antibody (1:50, Proteintech, IL, USA, 20960-1-AP) and anti-beta actin antibody (1:50, Abcam, Cambridge, UK, ab8227).

Detection of subcellular localization of PpIX. Intracellular accumulation of PpIX was detected using a confocal laser scanning microscope (LSM880; Carl Zeiss, Jena, Germany), according to a modified method (10,13). Briefly, lymphoma cells were seeded into a 35-mm flask culture in fresh medium containing 1 μM 5-ALA and incubated in the dark at 37˚C for 4 h. The cells were re-suspended in PBS/FBS, seeded in glass-bottom dishes (Asahi Techno Glass, Tokyo, Japan), and observed immediately. PpIX fluorescence (excitation, 488 nm; emission, 630-nm long-pass filter) was imaged using a confocal laser-scanning microscope. All procedures were performed in the dark.

Evaluation of cell responses to ionizing irradiation. Lymphoma cell lines were seeded at a density of $1x10^6$ cells/well in 6-well plates. Cells in hypoxic groups were exposed to hypoxic conditions by placing the appropriate plates in a multi-gas incubator with 5% O_2 for 24 h before the IR treatment. Cells in the 5-ALA treatment group were cultured in a complete medium containing 0.3 μM 5-ALA for 4 h. The plates were stored in a light-protected humid field chamber to avoid photoactivation of 5-ALA-induced PpIX. Cells were exposed to 2 Gy of IR using a gamma irradiator (Gammacell 40 Extractor; Nordion International, Inc., Ontario, Canada) at a dose-rate of 0.6 Gy/min. Cells under hypoxic conditions were maintained at 5% O_2 during IR exposure. The response of cells to IR was evaluated using a colony-forming assay. After 8-10 days of IR exposure, the cells were stained with a Thiazolyl Blue tetrazolium bromide solution. Three culture dishes were prepared for each group, and each experiment was performed independently three times. Only the colonies containing ≥50 cells were counted. The plating efficiency was determined for the unirradiated controls that were treated in the same way and maintained under the same conditions. Finally, the relative survival rates were calculated for each group.

Evaluation of intracellular levels of ROS after ionizing irradiation in lymphoma cells. Intracellular production of ROS immediately (0 h) and 12 h after IR was assessed using DCFD, an oxidant-sensitive fluorescent probe, using a flow cytometer. Cells were seeded in 35-mm culture flasks and irradiated with 8 Gy in the dark using a gamma irradiator. During the irradiation treatment, the culture flasks were kept in the dark at room temperature. Control cells were treated using the same procedure, but without exposure to 5-ALA and IR. Cells in the hypoxia groups were kept under 5% hypoxic conditions during IR exposure, treated in the same way, and maintained under the same conditions as the normoxic groups after IR. Cells in the 5-ALA group were treated with 0.3 μM 5-ALA for 4 h and then immediately exposed to IR. To evaluate intracellular level of ROS immediately after IR and after 12 h, each cell was re-suspended in 10 μM of DCFD solution after IR and incubated at 37˚C for 15 min before analysis. Then, DCFD fluorescence was analyzed using a flow cytometer (excitation, 488 nm; emission, 525/50 nm band-pass filter), as described above. All procedures were conducted in the dark. Analyses of flow cytometric data were performed using FlowJo software. In addition, the MFI of DCFD for treated cells relative to that of control cells was calculated for each cell line using FlowJo software.

Evaluation of mitochondrial density in lymphoma cells. Lymphoma cells were seeded into 35-mm glass-base dish in fresh medium containing 50 nM MitoTracker working solution and incubated in the dark at 37˚C for 30 min. To stain the nuclei, NucBlue was added to the dish and incubated under the same conditions for 15 min. MitoTracker (excitation, 488 nm; emission, 630-nm long-pass filter) and NucBlue (excitation, 405 nm; emission, 405/488 nm band-pass filter) fluorescence were imaged using a confocal laser scanning microscope. All procedures were performed in the dark. Mitochondrial density in lymphoma cells was calculated using microdensitometry. Based on previous studies (11,21), microdensitometry for quantitative evaluation of mitochondrial density in lymphoma cells was performed on these images using the public domain software ImageJ 1.53e (National Institute of Health, Bethesda, MD, USA), with modifications to the original methods. Briefly, the image data of all samples, including mitochondria and nuclear fluorescence images, were transferred to ImageJ. The 'freehand' tool was used to delineate the whole cell and nucleus and then measure the areas of the whole cell and nucleus, respectively. The cytosol areas were calculated by subtracting the areas of the nuclei from those of the whole cells. Next, the mitochondrial fluorescence image was converted to an 8-bit grayscale image using ImageJ. The freehand tool was then used to delineate the whole cell as the region of interest (ROI), and the mean gray value (MGV) of the mitochondrial fluorescence within the ROI was plotted on a graph. Finally, mitochondrial density was calculated by dividing the MGV of mitochondrial fluorescence by the area of the cytosol.

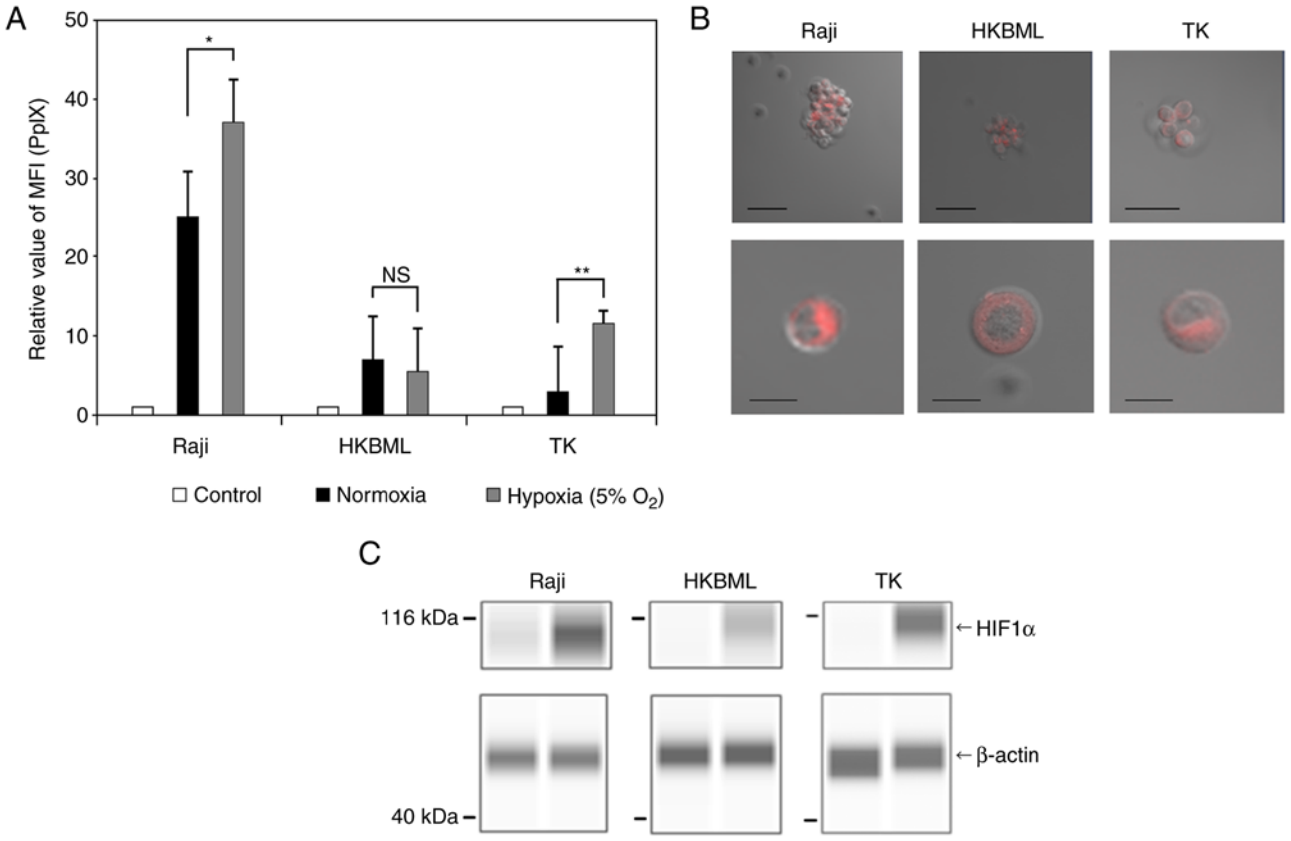

Figure 1. Intracellular accumulation and visualization of 5-ALA-induced PpIX in lymphoma cells. The intracellular PpIX fluorescence in lymphoma cells was determined using flow cytometry. Lymphoma cells were treated with 0.3 mM 5-ALA and incubated for 4 h. Hypoxic conditions were induced by placing cells in a multi-gas incubator (5% O_2) for 24 h before the treatment with 5-ALA, and expression analysis of HIF1α. (A) The relative MFI of 5-ALA-induced PpIX fluorescence was relative to that of 5-ALA-untreated cells in each cell line, and the relative MFI of 5-ALA-induced PpIX was compared under normoxic and hypoxic conditions. The control group was treated without 5-ALA under normoxic conditions. Columns, mean (n=8); error bars, SE. (B) Visualization of intracellular PpIX in the lymphoma cells treated with 1.0 mM 5-ALA for 4 h using a confocal laser scanning microscope (excitation, 488 nm; emission, 630-nm long-pass filter). Scale bar, 50 μm (top row) or 10 μm (bottom row). (C) Expression analysis of HIF1α in lymphoma cells. HIF1α and β-actin were detected using capillary western blotting, and the results are shown as capillary western lane view images which were obtained using the Simple Western system. *P<0.05; **P<0.01. 5-ALA, 5-aminolevulinic acid; HIF1α, hypoxia-induced factor 1α; MFI, median fluorescence intensity; NS, not significant; PpIX, protoporphyrin IX.

Statistical analysis. Data are presented as the means ± standard error (SE) of the mean. Statistical analyses were performed using EZR version 1.54 (https://www.jichi.ac.jp/saitama-sct/SaitamaHP.files/statmed.html), which is a graphical user interface for R version 4.0.3 (https://cran.r-project.org/) and R commander 2.7-1 (https://socialsciences.mcmaster.ca/jfox/Misc/Rcmdr/). The relative MFI of the PpIX fluorescence, and the survival rate of cells in the colony forming assay were analyzed using unpaired Student's t-tests. The relative MFI of the DCFD fluorescence (ROS) and the mitochondrial density were analyzed with a one-way analysis of variance followed by Bonferroni's test. A P-value of <0.05 was considered to indicate statistical significance (*P<0.05, **P<0.01)

Results

Evaluation of accumulation of 5-ALA-induced PpIX in lymphoma cells. We first examined the intracellular accumulation of 5-ALA-induced PpIX under normoxic and hypoxic conditions using flow cytometric analyses of the lymphoma cells (Figs. 1A and S1). The relative MFI of PpIX fluorescence in the 5-ALA-treated cells was obviously increased compared to that in the 5-ALA-untreated group in each cell line, with some variations. The relative MFI of PpIX fluorescence (mean ± SE) was 26.9±2.69 in the Raji line, 8.04±0.97 in the HKBML line, and 5.35±1.2 in the TK line under the normoxic conditions, respectively. Under the hypoxic conditions, the relative MFI of PpIX fluorescence (mean ± SE) was 35.9±2.97 in the Raji line, 7.04±1.42 in the HKBML line, and 14.28±2.66 in the TK line, respectively. In the Raji and TK lines, the relative MFI of PpIX fluorescence under the hypoxic conditions was significantly higher than that under the normoxic conditions (P<0.05 in Raji, and P<0.01 in TK). However, there was no significant difference in PpIX fluorescence between the conditions for HKBML (P=0.57). In the imaging examination of 5-ALA-induced PpIX, we confirmed PpIX accumulation in the 5-ALA-treated lymphoma cells using a confocal laser scanning microscope (LSM880, Zeiss). PpIX fluorescence accumulated densely in the cytoplasm but not in the nucleus of each cell line (Fig. 1B). Further, to evaluate the effect of the hypoxic conditions on each cell line, we confirmed the expression of HIF-1a using a Simple Western system. All cells showed induction of HIF-1a under 5% O_2 conditions (Fig. 1C).

Evaluation of efficacy of radiodynamic therapy with 5-ALA in lymphoma cells in vitro. We evaluated the efficacy of RDT

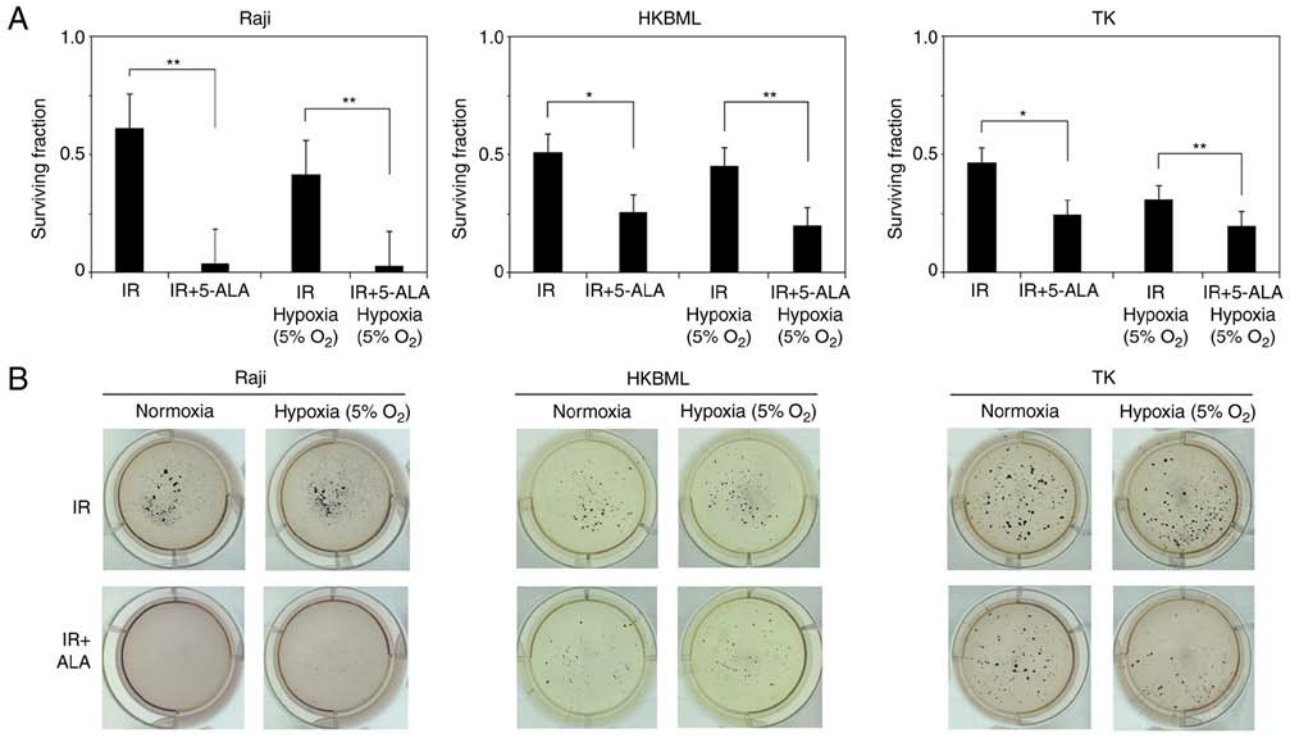

Figure 2. Evaluation of the radiodynamic effect of 5-ALA under normoxic and hypoxic conditions using standard colony formation assays in lymphoma cells *in vitro*. (A) Surviving fraction of lymphoma cells after radiodynamic therapy with 5-ALA under normoxic and hypoxic conditions. Columns, mean (n=9); error bars, SE. Cells were pre-treated with 5-ALA and exposed to IR. The total dose of IR was 2 Gy in each group. (B) Representative culture plate images from a standard colony formation assay in lymphoma cells. Cells without 5-ALA before IR (top) and cells pre-treated with 0.3 mM 5-ALA before IR (bottom). Colonies were stained using a blue tetrazolium bromide solution. *P<0.05; **P<0.01. 5-ALA, 5-aminolevulinic acid; IR, ionizing irradiation.

with 5-ALA in lymphoma cells using a colony-forming assay (Fig. 2). The relative survival rate of cells in 5-ALA treated group (mean ± SE) were significantly decreased compared with that in the 5-ALA-untreated group (0.61±0.08 vs. 0.04±0.01, P<0.01 for the Raji line; 0.51±0.08 vs. 0.26±0.03, P<0.05 for the HKBML line; 0.47±0.07 vs. 0.25±0.02, P<0.05 for the TK line, 5-ALA-untreated group vs. 5-ALA treatment group, respectively) under the normoxic conditions. Similarly, under the hypoxic conditions, the relative survival rate of the cells in 5-ALA treatment group was significantly decreased compared with that in the 5-ALA-untreated group (0.41±0.03 vs. 0.03±0.01, P<0.01 for the Raji line; 0.45±0.07 vs. 0.2±0.01, P<0.01 for the HKBML line; 0.31±0.03 vs. 0.2±0.01, P<0.01 for the TK line, 5-ALA-untreated group vs. 5-ALA treatment group, respectively). Thus, 5-ALA had a radiodynamic effect on the lymphoma cells under both normal and hypoxic conditions.

Temporal changes of ROS production following RDT with 5-ALA in vitro. We evaluated temporal changes in intracellular ROS production after IR in lymphoma cells under the normoxic and hypoxic conditions (Fig. 3A). In the cells without 5-ALA treatment, under the normoxic condition, the relative MFI of DCFD fluorescence (mean ± SE) 12 h after IR was significantly increased compared to that immediately after IR (0 h) in each cell line (1.04±0.04 vs. 1.71±0.09, P<0.01 in the Raji line; 0.93±0.03 vs. 1.13±0.04, P<0.01 in the HKBML line; 1.02±0.02 vs. 1.37±0.06, P<0.01 in the TK line; IR (0) vs. IR (12), respectively) (Figs. 3B, and S2 and S3). Thus, we confirmed that intracellular ROS production increased over time after IR without 5-ALA treatment in lymphoma cells, which is in agreement with previous reports (10,13,22,23). Meanwhile, the relative MFI of DCFD fluorescence (mean ± SE) in the 5-ALA treatment group was significantly higher than that in the 5-ALA-untreated group 12 h after IR in each cell (1.71±0.09 vs. 1.96±0.03, P<0.05 in the Raji line; 1.13±0.04 vs. 1.38±0.04, P<0.01 in the HKBML line; 1.37±0.06 vs. 1.57±0.04, P<0.05 in the TK line; 5-ALA-untreated group vs. 5-ALA treatment group, respectively). Thus, under normoxic conditions, the ROS production in the 5-ALA treatment group was significantly increased compared to that in the 5-ALA-untreated group 12 h after IR (Figs. 3B, S2 and S3).

In the 5-ALA-untreated cells under the hypoxic condition, the relative MFI of DCFD fluorescence (mean ± SE) 12 h after IR was significantly increased compared to that immediately after IR (0 h) in the Raji and TK cell lines (1.22±0.07 vs. 2.22±0.13, P<0.01 in the Raji cell line; 1.26±0.05 vs. 1.63±0.07, P<0.01 in the cell TK line; IR (0) vs. IR (12), respectively) (Figs. 3C, S2A and C, and S3). There was no significant difference in the relative MFI of DCFD fluorescence (mean ± SE) of the 5-ALA-untreated group between immediately after IR (0 h) and 12 h after IR in the HKBML cell line (1.07±0.03 vs. 1.28±0.05, P>0.05) (Figs. 3C, and S2B and S3). The relative MFI of DCFD fluorescence (mean ± SE) in the 5-ALA treatment group was significantly higher than that in the 5-ALA-untreated group 12 h after IR in the TK cell line (1.63±0.07 vs. 1.91±0.09, P<0.05) (Figs. 3C and S2C and S3). There was no significant difference in the relative MFI of DCFD fluorescence (mean ± SE) 12 h after IR between the 5-ALA-untreated group and the 5-ALA treatment group in the

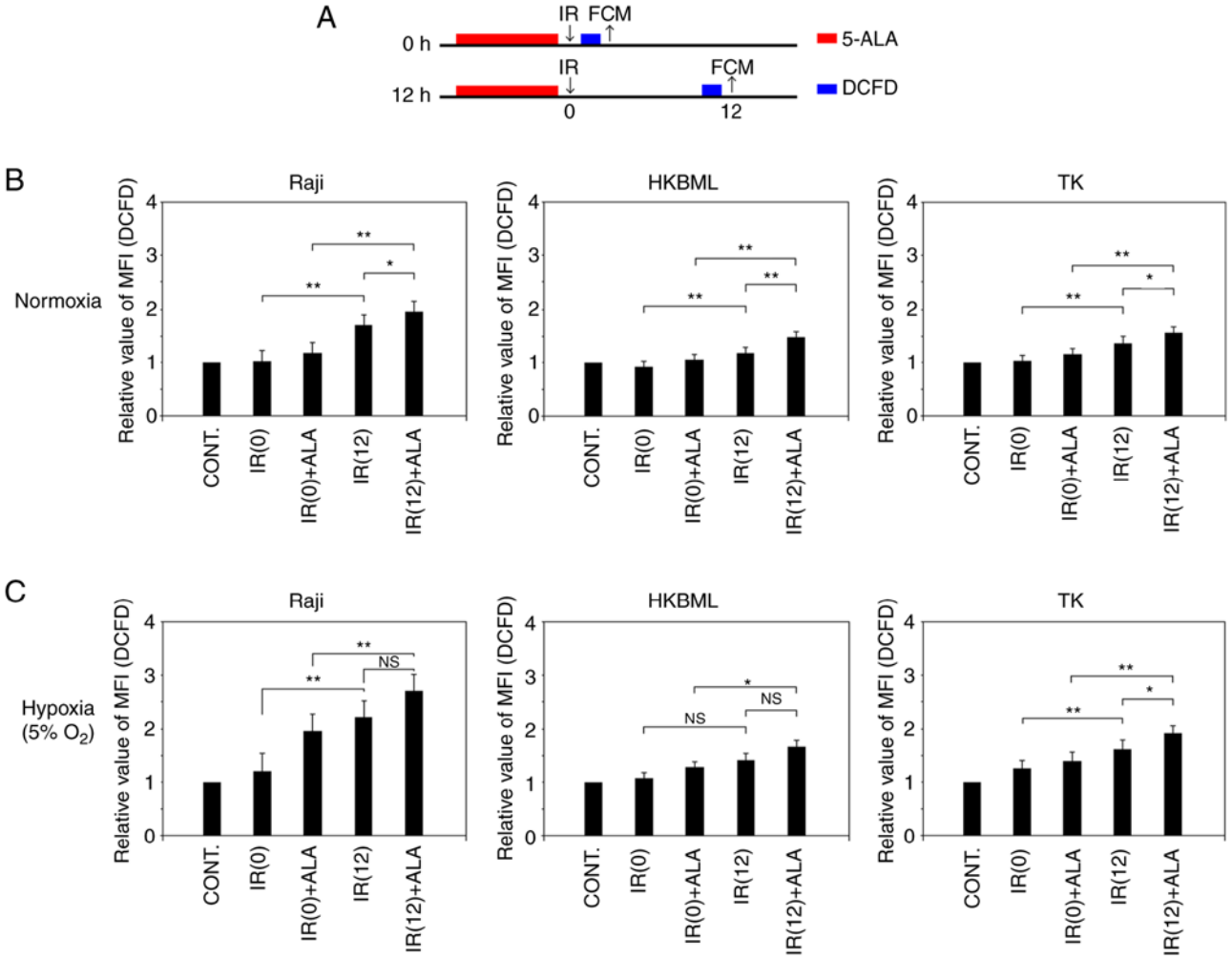

Figure 3. Temporal changes of ROS production in radiodynamic therapy with 5-ALA *in vitro*. (A) Schedules of the 5-ALA treatment, exposure to IR and detection of ROS procedures. Cells were incubated with 0.3 mM 5-ALA for 4 h. Hypoxic conditions were induced by placing cells in a multi-gas incubator (5% O_2) for 24 h before the treatment, and then, cells were kept in hypoxic conditions during IR. Detection of ROS was conducted using an oxidant-sensitive fluorescent probe (DCFD). The control values were the intracellular ROS levels in the cells without 5-ALA treatment or exposure to IR. The MFI of DCFD fluorescence in the cells after IR exposure in relation to that of the control was calculated in each cell line and then, the relative MFI of DCFD fluorescence was compared in the cells immediately and 12 h after IR. Relative MFI of DCFD fluorescence (intracellular ROS levels) after IR in lymphoma cells under (B) normoxic and (C) hypoxic conditions. Columns, mean (n=5); error bars, SE. *P<0.05; **P<0.01. 5-ALA, 5-aminolevulinic acid; CONT, control; DCFD, 2CM-H_2DCFDA; FCM, flow cytometry; IR, ionizing irradiation; MFI, median fluorescence intensity; NS, not significant; ROS, reactive oxygen species; IR (0), cells immediately after IR but without 5-ALA treatment; IR (12), cells 12 h after IR but without 5-ALA treatment; IR(0) + ALA, cells immediately after IR with 5-ALA pretreatment; IR(12) + ALA, cells 12 h after IR with 5-ALA pretreatment.

Raji and HKBML cell lines (2.22±0.13 vs. 2.72±0.24, P>0.05 in the Raji cell line; 1.28±0.05 vs. 1.51±0.08, P>0.05 in the HKBML cell line; 5-ALA-untreated vs. 5-ALA treatment group, respectively) (Figs. 3C, S2A and B, and S3). Thus, under hypoxic conditions, only TK cells exhibited significantly increased ROS production in the 5-ALA treatment group compared with the 5-ALA-untreated group 12 h after IR.

Evaluation of mitochondrial density in lymphoma cells. We evaluated the mitochondrial density in lymphoma cells using microdensitometry with mitochondrial and nuclear staining through confocal laser scanning microscopy (Fig. 4A). The mitochondrial density (mean ± SE) was 0.78±0.05 in the Raji line, 0.55±0.04 in the HKBML line, and 0.5±0.06 in the TK line, respectively (Fig. 4B). The mitochondrial density in the Raji cells was significantly higher than that in the HKBML and TK cells (P<0.01) (Fig. 4B).

Discussion

We previously demonstrated that 5-ALA enhances oxidative stress and delayed ROS production in mitochondria after IR, and enhances cell death in proportion to 5-ALA-induced PpIX accumulation in glioma cells *in vitro* (10,13). In addition, we confirmed that 5-ALA enhanced the host antitumor immune response and caused high inhibition of tumor growth in a rat subcutaneous glioma model (11). Similarly, the present study demonstrated that 5-ALA resulted in high PpIX accumulation and enhanced cell death, with an increase in delayed ROS production after IR in lymphoma cells. To the best of our knowledge, this is the first study to investigate the radiodynamic effect of 5-ALA on lymphoma cells.

Although many recent studies have demonstrated the radiodynamic effect of 5-ALA in tumor cells (14-16,18), the appropriate conditions for RDT with 5-ALA remain unclear.

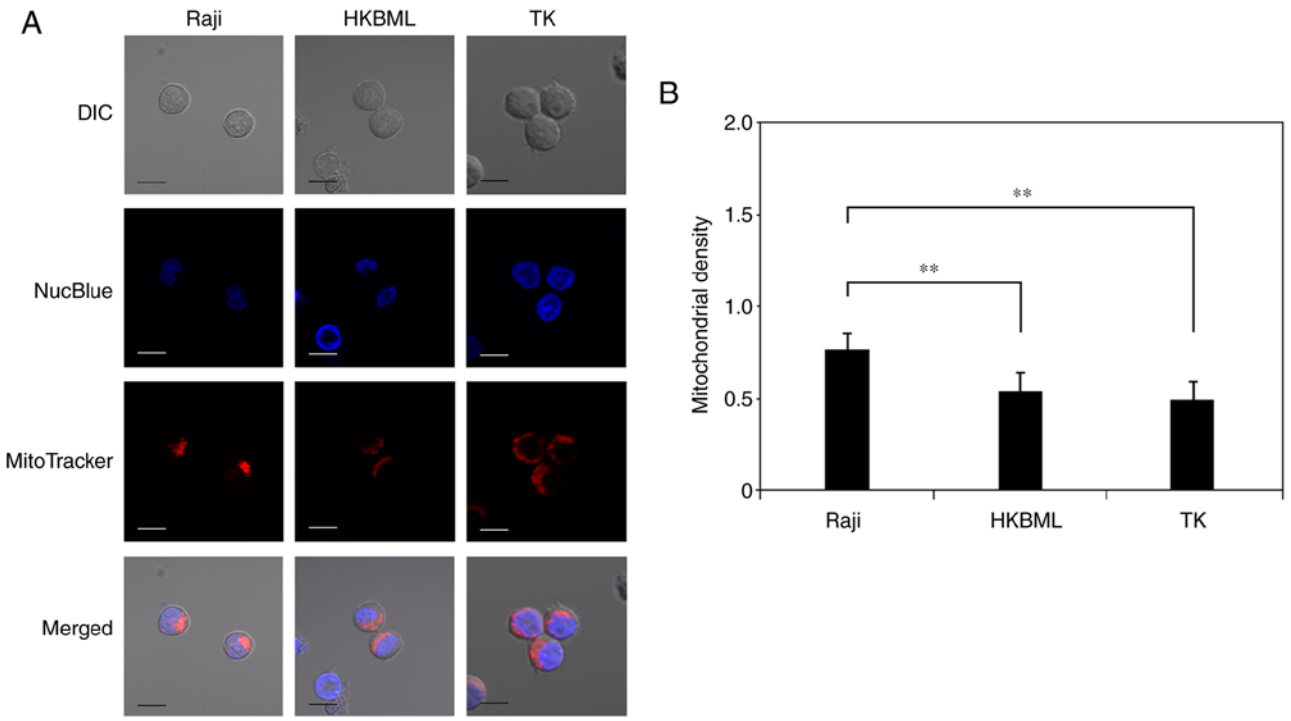

Figure 4. Evaluation of the mitochondrial density in lymphoma cells. (A) Visualization of nuclei and mitochondria in lymphoma cells using a confocal laser scanning microscope. Cells were treated with NucBlue to identify the nuclei and with MitoTracker to identify mitochondria. The merged image included the NucBlue fluorescence and MitoTracker fluorescence staining, and the DIC image. Scale bar, 10 μm. (B) Mitochondrial density in lymphoma cells as determined using microdensitometric analysis using ImageJ. Columns, mean (n=4); error bars, SE. **P<0.01. DIC, differential interference contrast.

In a prior study, we performed 5-ALA/RDT with 2 Gy/day for five consecutive days (total 10 Gy) in a rat glioma subcutaneous model, then confirmed the inhibition of tumor growth with strong aggregation of Iba-1 positive macrophages within the tumor specimen (11). Another recent study performed 5-ALA/RDT with 2 Gy/day for five consecutive days x2 courses (total 20 Gy) in a mouse melanoma subcutaneous tumor model and demonstrated the radiodynamic effect of 5-ALA via tumor growth curve creation and microarray analysis of the gene expression profiles in tumor specimens (14). Another study also demonstrated the radiodynamic effect of 5-ALA at 4 Gy/day for three consecutive days (total 12 Gy) in a mouse subcutaneous tumor model inoculated with prostate cancer cells (16). That study reported reductions in tumor volumes and mitotic activities by comparing the pathological findings in a 5-ALA/RDT group and a control group. In addition, they demonstrated that radiosensitization by 5-ALA was not due to the photodynamic effect of light contamination by examining subcutaneous tumors covered with high-performance black masking tape (16). In contrast, a recent study investigated the radiodynamic effect of 5-ALA using a mouse brain tumor model inoculated with patient-derived glioblastoma stem cells (24). They performed 5-ALA/RDT at 2 Gy/day five times (3 times a week, Monday/Wednesday/Friday; total 10 Gy) and evaluated tumor volume using luciferin-based bioluminescence imaging (24). However, the bioluminescence of the brain tumors in the 5-ALA/RDT group varied widely, and consequently, they could not demonstrate the radiodynamic effect of 5-ALA in their mouse brain tumor model (24).

In terms of the oxidative stress in the mitochondria of tumor cells, it may be important to increase ROS production over the lethal level through different treatments (25). We confirmed that ROS production after 5-ALA/RDT increased over time (within 12 h) in glioma and lymphoma cell lines under the normoxic condition, including in the present study (10,13). Meanwhile, a study utilizing prostate cancer cells revealed that ROS production increased just after 5-ALA/RDT and then gradually decreased over time (within 12 h) (26). Thus, the pattern of ROS production after 5-ALA/RDT treatment varied in each cell line. Once oxidative stress damages the mitochondria within tumor cells, impaired mitochondria produce ROS via metabolic processes (22,23). However, if these ROS do not reach a lethal level, the impaired mitochondria may recover with time (more than 24 h), and then the ROS production will gradually decrease (23). Consequently, the mitochondria may regain normal function. Because the radiodynamic effect of 5-ALA through single-dose IR is weak (12), the duration of each fraction of IR may be important in RDT with 5-ALA. Taken together, we hypothesize that IR exposure is needed before impaired mitochondria completely regain their ability to produce ROS above lethal levels during 5-ALA/RDT. Namely, the duration of each fraction of IR is recommended to be within 24 h following 5-ALA/RDT. Recently, clinicians have considered the application of RDT with 5-ALA as an adjuvant therapy for patients (27-29). Thus, further studies are required to determine the appropriate conditions of IR in 5-ALA/RDT.

Tumor hypoxia is associated with poor clinical outcomes in many cancers, and hypoxic tumor cells are up to three times more resistant to radiotherapy than normoxic tumor cells owing to the absence of the oxygen enhancement effect (30,31). Even very low levels of oxygen (approximately

2%) are sufficient to yield an oxygen enhancement effect in radiotherapy (32), and many studies have defined oxygen levels of 1-5% as hypoxic conditions *in vitro* (26,33,34). First, we confirmed that the cell culture was unstable under hypoxic conditions of 1% O_2 in our experimental setting. Thus, in the present study, we cultured cells in 5% O_2 and confirmed the induction of HIF-1a in each cell line. 5-ALA accumulated PpIX, and radiotherapy with 5-ALA clearly inhibited cell proliferation compared to radiotherapy alone in colony formation assay under hypoxic conditions in lymphoma cells. In the present study, lymphoma cells revealed different survival rates in 5-ALA/RDT in each cell line, with some variation. 5-ALA is metabolized and converted to heme in the mitochondria via the heme synthesis in normal cells (5). In tumor cells, the heme synthesis is stopped at the final step, and PpIX is not converted to heme, which leads to accumulation of PpIX in the mitochondria of tumor cells (5). Therefore, the accumulation of 5-ALA-induced PpIX is dependent on the cell metabolism in tumor cells (5). In the present study, lymphoma cells exhibited differences in 5-ALA-induced PpIX accumulation under different oxygen culture conditions. In addition, only TK cells exhibited enhancement of ROS production 12 h after IR in the 5-ALA-treated group under hypoxic conditions. Although further studies evaluating the effect of 5-ALA on ROS production after IR under hypoxic conditions are required, these differences may depend on the amount of 5-ALA-induced PpIX accumulation and mitochondrial density. A recent study demonstrated that 5-ALA/RDT induced an increase in mitochondrial ROS production and conversion of mitochondria-mediated tumor metabolism into quiescent status via the inhibition of HIF-1, the mitochondrial oxygen consumption rate (OCR), and the extracellular acidification rate, and then it inhibited cancer stemness under hypoxic conditions. Finally, 5-ALA helped prostate cancer cells overcome the effects of hypoxia-induced radiation resistance (26). Although reoxygenation of the cell culture cannot be completely excluded, we believe that 5-ALA can induce a radiodynamic effect in lymphoma cells under hypoxic conditions.

DLBCLs exhibit highly heterogeneous metabolic features, such as BCR-dependent and OxPhos-DLBCLs (35). BCR-dependent subtype has greater glycolytic flux, typical of the Warburg phenotype. Meanwhile, OxPhos-subtype shows elevated electron transport chain activity, ATP production, and fatty acid oxygenation. In addition, these metabolic phenotypes are associated with a subtype selective survival mechanism (35). Considering the mechanism of the radiodynamic effect of 5-ALA, 5-ALA-induced PpIX is a key mediator, not 5-ALA itself. The cell metabolism affects the conversion of 5-ALA into PpIX. In tumor cells, 5-ALA treatment is associated with accumulation of PpIX in the mitochondria due to the mitochondrial dysfunction, including inactivation of heme converted enzyme (5). As previous studies demonstrated, 5-ALA-induced PpIX enhanced the antitumor effect induced by radiotherapy in tumor cells (5,10-18). In the present study, lymphoma cells showed differences in ROS production after IR and 5-ALA-induced PpIX accumulation under hypoxic conditions in each cell line. Accumulation of 5-ALA-induced PpIX in Raji and TK cells but not HKBML cells under hypoxic conditions was significantly increased compared with that under normoxic conditions according to flow cytometric analysis. In addition, only in TK cells, ROS production was increased 12 h after IR in 5-ALA treated cells under hypoxic conditions. Taken together, the differences in 5-ALA metabolism under different oxygen conditions may affect the 5-ALA-induced PpIX accumulation and ROS production after IR in lymphoma cells. A further study of the metabolic changes within lymphoma cells in the surrounding environment is needed. According to a recent clinical study using physiologic magnetic resonance imaging, tumor microenvironment mapping of patients demonstrated intertumoral heterogeneity factors such as 65% glycolysis, 19% OxPhos, 9% hypoxia, and 7% necrosis in PCNSL (36). Thus, recent therapeutic strategies have been developed for each metabolic target in DLBCL (37,38). Although further investigations are required, 5-ALA/RDT may become a treatment option for PCNSL.

5-ALA has been widely used in clinical settings as a live molecular marker for glioma and PCNSL (8,39), and many experimental studies have demonstrated the radiodynamic effect of 5-ALA in cancer cells. Nevertheless, the precise mechanism of action of 5-ALA/RDT remains unclear. Recently, IR has been shown to affect both the nucleus and mitochondria, which includes activation of the DNA damage response and mitochondrial signaling toward apoptosis (40). Importantly, impaired mitochondria damaged by IR produce ROS (mainly superoxide) via the metabolic process, then damage the rest of the surrounding normal mitochondria, consequently propagating oxidative stress within the cell, which is denoted as '*intermitochondrial communication*' (41). This effect amplifies the oxidative damage signal and further metabolic ROS production over time after IR. In addition, a recent study demonstrated that mitochondria damaged by IR activated an immune response in the nucleus (42).

PpIX enhances the production of ROS such as superoxide, hydroxyl radicals, and singlet oxygen via water radiolysis induced by IR (9), and 5-ALA accumulates PpIX in the mitochondria of cancer cells. In a previous study, we confirmed that 5-ALA treatment after IR did not enhance ROS production in glioma cells (13). In the present study, the Raji line revealed a high accumulation of 5-ALA-induced PpIX and a high 5-ALA/RDT effect compared to the other cell lines. Therefore, we propose that focal oxidative stress in the mitochondria is the first step, and high accumulation of PpIX in the mitochondria is important just before IR exposure in 5-ALA/RDT. In future studies, oxidative stress in cancer cells after IR in 5-ALA/RDT should be examined in detail.

Although the pattern of ROS production after IR varies, we hypothesized that continuous oxidative stress above the lethal level after IR in 5-ALA/RDT is important, which is in agreement with another study (26). Namely, delayed ROS production via effective '*intermitochondrial communication*' may enhance the therapeutic effects during 5-ALA/RDT. Thus, we speculated that '*intermitochondrial communication*' was dependent on the distance between each mitochondrion and examined the mitochondrial density in lymphoma cells. In the present study, the Raji cells showed significantly higher mitochondrial density values than the other cells. As we described previously, we recently noticed the importance of the application of 5-ALA/RDT for radiosensitive malignant neoplasms. We, therefore, began this experimental *in vitro*

study using lymphoma cell lines. Although the mechanism of 5-ALA/RDT is complicated, we believe that the mitochondria play a main role in this process, and further investigation of the mitochondrial response is required, including their roles in the apoptotic signaling, metabolism, and dynamics of 5-ALA/RDT, and the experimental tumor model in lymphoma.

This study has certain limitations. We confirmed the radiodynamic effect of 5-ALA in lymphoma cells *in vitro*, but not in an *in vivo* study. We have ever investigated the radiodynamic effect of 5-ALA using a rat allogeneic subcutaneous tumor model inoculated with 9L gliosarcoma, and confirmed enhancement of the host antitumor immune response. It is possible that, in an *in vivo* study of lymphoma, host immunity may affect the results of 5-ALA/RDT.

In conclusion, 5-ALA has been widely used as a fluorescent live marker for glioma and PCNSL in clinical settings. Although PCNSL is radiosensitive, reduction of the radiation dose is needed to avoid delayed radiation injury while maintaining therapeutic effects, particularly in the elderly. 5-ALA accumulates PpIX and induces a radiodynamic effect in lymphoma cells under both normoxic and hypoxic conditions. Thus, 5-ALA/RDT is a potential therapeutic option for PCNSL.

Acknowledgements

Not applicable.

Funding

This work was supported by JSPS KAKENHI (grant no. 18K07307).

Availability of data and materials

The datasets used and/or analyzed during the current study are available from the corresponding author on reasonable request.

Authors' contributions

KS and JY drafted the final manuscript. KS, JY, KT and RM made substantial contributions to the conception and design of the study. KS, JY, KT and RM critically revised the manuscript and provided constructive feedback. KS, KT and RM performed flow cytometric analysis and interpreted the data. KS and JY performed fluorescence cell imaging and interpreted the data. KS, JY and RM confirm the authenticity of the raw data. All authors have read and approved the final manuscript.

Ethics approval and consent to participate

Not applicable.

Patient consent for publication

Not applicable.

Competing interests

The authors declare that they have no competing interests.

References

1. Han CH and Batchelor TT: Diagnosis and management of primary central nervous system lymphoma. Cancer 123: 4314-4324, 2017.
2. Siegal T and Bairey O: Primary CNS lymphoma in the elderly: The challenge. Acta Haematol 141: 138-145, 2019.
3. Ferreri AJ and Marturano E: Primary CNS lymphoma. Best Pract Res Clin Haematol 25: 119-130, 2012.
4. Calimeri T, Steffanoni S, Gagliardi F, Chiara A, and Ferreri AJM: Erratum to 'How we treat primary central nervous system lymphoma': [ESMO Open Volume 6, Issue 4, August 2021, 100213]. ESMO Open 6: 100326, 2021.
5. Ishizuka M, Abe F, Sano Y, Takahashi K, Inoue K, Nakajima M, Kohda T, Komatsu N, Ogura S and Tanaka T: Novel development of 5-aminolevurinic acid (ALA) in cancer diagnoses and therapy. Int Immunopharmacol 11: 358-365, 2011.
6. Stummer W, Pichlmeier U, Meinel T, Wiestler OD, Zanella F and Reulen HJ; ALA-Glioma Study group: Fluorescence-guided surgery with 5-aminolevulinic acid for resection of malignant glioma: A randomised controlled multicentre phase III trial. Lancet Oncol 7: 392-401, 2006.
7. Stummer W, Holling M, Bendok BR, Vogelbaum MA, Cox A, Renfrow SL, Widhalm G, Ezrin A, DeSena S, Sackman ML and Wyse JW: The NXDC-MEN-301 Study on 5-ALA for meningiomas surgery: An innovative study design for the assessing the benefit of intra-operative fluorescence imaging. Brain Sci 12: 1044, 2022.
8. Kiesel B, Millesi M, Woehrer A, Furtner J, Bavand A, Roetzer T, Mischkulnig M, Wolfsberger S, Preusser M, Knosp E and Widhalm G: 5-ALA-induced fluorescence as a marker for diagnostic tissue in stereotactic biopsies of intracranial lymphomas: Experience in 41 patients. Neurosurg Focus 44: E7, 2018.
9. Takahashi J and Misawa M: Characterization of reactive oxygen species generated by protoporphyrin IX under X-ray irradiation. Radiat Phys Chem 78: 889-898, 2009.
10. Ueta K, Yamamoto J, Tanaka T, Nakano Y, Kitagawa T and Nishizawa S: 5-Aminolevulinic acid enhances mitochondrial stress upon ionizing irradiation exposure and increases delayed production of reactive oxygen species and cell death in glioma cells. Int J Mol Med 39: 387-398, 2017.
11. Yamamoto J, Ogura S, Shimajiri S, Nakano Y, Akiba D, Kitagawa T, Ueta K, Tanaka T and Nishizawa S: 5-aminolevulinic acid-induced protoporphyrin IX with multi-dose ionizing irradiation enhances host antitumor response and strongly inhibits tumor growth in experimental glioma in vivo. Mol Med Rep 11: 1813-1819, 2015.
12. Yamamoto J, Ogura S, Tanaka T, Kitagawa T, Nakano Y, Saito T, Takahashi M, Akiba D and Nishizawa S: Radiosensitizing effect of 5-aminolevulinic acid-induced protoporphyrin IX in glioma cells in vitro. Oncol Rep 27: 1748-1752, 2012.
13. Kitagawa T, Yamamoto J, Tanaka T, Nakano Y, Akiba D, Ueta K and Nishizawa S: 5-Aminolevulinic acid strongly enhances delayed intracellular production of reactive oxygen species (ROS) generated by ionizing irradiation: Quantitative analyses and visualization of intracellular ROS production in glioma cells in vitro. Oncol Rep 33: 583-590, 2015.
14. Takahashi J, Murakami M, Mori T and Iwahashi H: Verification of radiodynamic therapy by medical linear accelerator using a mouse melanoma tumor model. Sci Rep 8: 2728, 2018.
15. Yamada K, Murayama Y, Kamada Y, Arita T, Kosuga T, Konishi H, Morimura R, Shiozaki A, Kuriu Y, Ikoma H, *et al*: Radiosensitizing effect of 5-aminolevulinic acid in colorectal cancer in vitro and in vivo. Oncol Lett 17: 5132-5138, 2019.
16. Miyake M, Tanaka N, Hori S, Ohnishi S, Takahashi H, Fujii T, Owari T, Ohnishi K, Iida K, Morizawa Y, *et al*: Dual benefit of supplementary oral 5-aminolevulinic acid to pelvic radiotherapy in a syngenic prostate cancer model. Prostate 79: 340-351, 2019.
17. Kaneko T, Tominaga M, Kouzaki R, Hanyu A, Ueshima K, Yamada H, Suga M, Yamashita T, Okimoto T and Uto Y: Radiosensitizing effect of 5-aminolevulinic acid and protoporphyrin IX on Carbon-ion beam irradiation. Anticancer Res 38: 4313-4317, 2018.
18. Yang DM, Cvetkovic D, Chen L and Ma CC: Therapeutic effects of in-vivo radiodynamic therapy (RDT) for lung cancer treatment: A combination of 15MV photons and 5-aminolevulinic acid (5-ALA). Biomed Phys Eng Express 8: 1088/2057-1976/ac9b5c, 2022.

19. Wang J, Valdez A and Chen Y: Evaluation of automated Wes system as an analytical and characterization tool to support monoclonal antibody drug product development. J Pharm Biomed Anal 139: 263-268, 2017.
20. Baddela VS, Sharma A, Michaelis M and Vanselow J: HIF1 driven transcriptional activity regulates steroidogenesis and proliferation of bovine granulosa cells. Sci Rep 10: 3906, 2020.
21. Prall F, Maletzki C and Linnebacher M: Microdensitometry of osteopontin as an immunohistochemical prognostic biomarker in colorectal carcinoma tissue microarrays: Potential and limitations of the method in 'biomarker pathology'. Histopathology 61: 823-832, 2012.
22. Yamamori T, Yasui H, Yamazumi M, Wada Y, Nakamura Y, Nakamura H and Inanami O: Ionizing radiation induces mitochondrial reactive oxygen species production accompanied by upregulation of mitochondrial electron transport chain function and mitochondrial content under control of the cell cycle checkpoint. Free Radic Biol Med 53: 260-270, 2012.
23. Saenko Y, Cieslar-Pobuda A, Skonieczna M and Rzeszowska-Wolny J: Changes of reactive oxygen and nitrogen species and mitochondrial functioning in human K562 and HL60 cells exposed to ionizing radiation. Radiat Res 180: 360-366, 2013.
24. Dupin C, Sutter J, Amintas S, Derieppe MA, Lalanne M, Coulibaly S, Guyon J, Daubon T, Boutin J, Blouin JM, *et al*: An orthotopic model of glioblastoma is resistant to radiodynamic therapy with 5-AminoLevulinic acid. Cancers (Basel) 14: 4244, 2022.
25. Galadari S, Rahman A, Pallichankandy S and Thayyullathil F: Reactive oxygen species and cancer paradox: To promote or to suppress? Free Radic Biol Med 104: 144-164, 2017.
26. Owari T, Tanaka N, Nakai Y, Miyake M, Anai S, Kishi S, Mori S, Fujiwara-Tani R, Hojo Y, Mori T, *et al*: 5-Aminolevulinic acid overcomes hypoxia-induced radiation resistance by enhancing mitochondrial reactive oxygen species production in prostate cancer cells. Br J Cancer 127: 350-363, 2022.
27. Nordmann NJ and Michael AP: 5-Aminolevulinic acid radiodynamic therapy for treatment of high-grade gliomas: A systematic review. Clin Neurol Neurosurg 201: 106430, 2021.
28. Krivoshapkin A, Gaytan A, Abdullaev O, Salim N, Sergeev G, Marmazeev I, Cesnulis E, Killeen T, Tyuryn V, Kiselev R, *et al*: Prospective comparative study of intraoperative balloon electronic brachytherapy versus resection with multidisciplinary adjuvant therapy for recurrent glioblastoma. Surg Neurol Int 12: 517, 2021.
29. Pepper NB, Stummer W and Eich HT: The use of radiosensitizing agents in the therapy of glioblastoma multiforme-a comprehensive review. Strahlenther Onkol 198: 507-526, 2022.
30. Higgins GS, O'Cathail SM, Muschel RJ and McKenna WG: Drug radiotherapy combinations: Review of previous failures and reasons for future optimism. Cancer Treat Rev 41: 105-113, 2015.
31. Dhani N, Fyles A, Hedley D and Milosevic M: The clinical significance of hypoxia in human cancers. Semin Nucl Med 45: 110-121, 2015.
32. Ashton TM, McKenna WG, Kunz-Schughart LA and Higgins GS: Oxidative phosphorylation as an emerging target in cancer therapy. Clin Cancer Res 24: 2482-2490, 2018.
33. Ihata T, Nonoguchi N, Fujishiro T, Omura N, Kawabata S, Kajimoto Y and Wanibuchi M: The effect of hypoxia on photodynamic therapy with 5-aminolevulinic acid in malignant gliomas. Photodiagnosis Photodyn Ther 40: 103056, 2022.
34. Castillo CA, Leon D, Ruiz MA, Albasanz JL and Martin M: Modulation of adenosine A1 and A2A receptors in C6 glioma cells during hypoxia: Involvement of endogenous adenosine. J Neurochem 105: 2315-2329, 2008.
35. Caro P, Kishan AU, Norberg E, Stanley IA, Chapuy B, Ficarro SB, Polak K, Tondera D, Gounarides J, Yin H, *et al*: Metabolic signatures uncover distinct targets in molecular subsets of diffuse large B cell lymphoma. Cancer Cell 22: 547-560, 2012.
36. Stadlbauer A, Marhold F, Oberndorfer S, Heinz G, Zimmermann M, Buchfelder M, Heynold E and Kinfe TM: Metabolic tumor microenvironment characterization of contrast enhancing brain tumors using physiologic MRI. Metabolites 11: 668, 2021.
37. Norberg E, Lako A, Chen PH, Stanley IA, Zhou F, Ficarro SB, Chapuy B, Chen L, Rodig S, Shin D, *et al*: Differential contribution of the mitochondrial translation pathway to the survival of diffuse large B-cell lymphoma subsets. Cell Death Differ 24: 251-262, 2017.
38. Noble RA, Thomas H, Zhao Y, Herendi L, Howarth R, Dragoni I, Keun HC, Vellano CP, Marszalek JR and Wedge SR: Simultaneous targeting of glycolysis and oxidative phosphorylation as a therapeutic strategy to treat diffuse large B-cell lymphoma. Br J Cancer 127: 937-947, 2022.
39. Farrell C, Shi W, Bodman A and Olson JJ: Congress of neurological surgeons systematic review and evidence-based guidelines update on the role of emerging developments in the management of newly diagnosed glioblastoma. J Neurooncol 150: 269-359, 2020.
40. Averbeck D and Rodriguez-Lafrasse C: Role of mitochondria in radiation responses: Epigenetic, metabolic, and signaling impacts. Int J Mol Sci 22: 11047, 2021.
41. Kam WW and Banati RB: Effects of ionizing radiation on mitochondria. Free Radic Biol Med 65: 607-619, 2013.
42. Tigano M, Vargas DC, Tremblay-Belzile S, Fu Y and Sfeir A: Nuclear sensing of breaks in mitochondrial DNA enhances immune surveillance. Nature 591: 477-481, 2021.